THE JOURNAL OF PHYSICAL CHEMISTRY A

A: Environmental, Combustion, and Atmospheric Chemistry; Aerosol Processes, Geochemistry, and Astrochemistry

Rapid Aqueous-Phase Hydrolysis of Ester Hydroperoxides Arising from Criegee Intermediates and Organic Acids

Ran Zhao, Christopher M Kenseth, Yuanlong Huang, Nathan F Dalleska, Xiaobi Michelle Kuang, Jierou Chen, Suzanne E Paulson, and John H. Seinfeld

J. Phys. Chem. A, **Just Accepted Manuscript** • DOI: 10.1021/acs.jpca.8b02195 • Publication Date (Web): 21 May 2018

Rapid Aqueous-Phase Hydrolysis of Ester Hydroperoxides Arising from Criegee Intermediates and Organic Acids

Ran Zhao,[*,†,‡] Christopher M. Kenseth,[†] Yuanlong Huang,[¶] Nathan F. Dalleska,[§] Xiaobi M. Kuang,[‖] Jierou Chen,[‖] Suzanne E. Paulson,[‖] and John H. Seinfeld[†,⊥]

†*Devision of Chemistry and Chemical Engineering, California Institute of Technology, Pasadena, CA, USA 91125*

‡*Now at: Department of Chemistry, University of Alberta, Edmonton, AB, Canada T6G 2G2*

¶*Division of Geological and Planetary Sciences, California Institute of Technology, Pasadena, CA, USA 91125*

§*Environmental Analysis Center, California Institute of Technology, Pasadena, CA, USA 91125*

‖*Department of Atmospheric and Oceanic Sciences, University of California - Los Angeles, Los Angeles, CA, USA 90095*

⊥*Division of Engineering and Applied Science, California Institute of Technology, Pasadena, CA, USA 91125*

E-mail: rzhao@caltech.edu

Phone: +1 626-395-8928

Abstract

Stabilized Criegee intermediates react with organic acids in the gas phase and at the air-water interface to form a class of ester hydroperoxides, α-acyloxyalkyl hydroperoxides (αAAHPs). A number of recent studies have proposed the importance of αAAHPs to the formation and growth of secondary organic aerosol (SOA). The chemistry of αAAHPs has not been investigated due to a lack of commercially available chemical standards. In this work, the behavior of αAAHPs in condensed phases is investigated for the first time. Experiments were performed with two synthesized αAAHP species. αAAHPs decomposed rapidly in the aqueous phase, with the rate highly dependent on the solvent, temperature, solution pH, and other compounds present in the solution. The measured 1^{st}-order decomposition rate coefficient varied between 10^{-3} s^{-1} and 10^{-5} s^{-1} under the conditions examined in this work. Elucidation of the reaction mechanism is complicated by byproducts arising from the synthetic procedure, but observations are consistent with a base-catalyzed hydrolysis of αAAHPs. The rapid hydrolysis of αAAHPs observed in this work implies their short lifetimes in ambient cloud and fog waters. Decomposition of αAAHPs likely gives rise to smaller peroxides, such as H_2O_2. The loss of αAAHPs is also relevant to filter extraction, which is commonly practiced in laboratory experiments, potentially explaining contradictory results reported in the existing literature regarding the importance of αAAHPs in SOA.

Introduction

Alkenes (e.g., isoprene and monoterpenes) comprise over half of the total volatile organic compounds (VOCs) emitted to Earth's atmosphere.[1] Owing to the reactivity of the C=C bond towards O_3, ozonolysis is a major sink of alkenes. Ozonolysis converts alkenes into oxygenated products that exhibit lower vapor pressures and contribute to the formation of secondary organic aerosol (SOA), a class of suspended organic particulate matter that affects air quality and global climate.[2] As shown in the generalized reaction scheme of alkene ozonolysis (Figure 1), O_3 first adds across the C=C bond, giving rise to a primary ozonide,

which decomposes to a carbonyl compound and an excited carbonyl oxide referred to as the Criegee intermediate.[3] The Criegee intermediate is presented as a zwitterion in Figure 1, as it is the most stable configuration,[4] but it is also commonly referred to as a biradical in the literature. The Criegee intermediate can either undergo unimolecular decomposition or be stabilized upon collision with air (i.e., N_2 and O_2). The stabilized Criegee intermediate (SCI) can react bimolecularly with a wide spectrum of molecules collectively known as Criegee scavengers, among which organic acids are particularly efficient.[4,5] The reaction between the C_1 SCI and formic acid proceeds nearly at the collision limit,[6] with a rate coefficient larger than that of SCI + H_2O by 3 to 4 orders of magnitude.[7–9] The product arising from the SCI + organic acid reaction is an ester hydroperoxide, α-acyloxyalkyl hydroperoxide (αAAHP, Figure 1).[10] A number of studies have proposed that αAAHPs can contribute to SOA mass due to their low volatility, and alternatively, they can react further with another SCI to form compounds with even lower volatilities.[6,11]

Monoterpenes comprise a major fraction of global biogenic VOC emissions,[1] and the reaction products of monoterpene SCIs are of great importance to atmospheric chemistry. Recent studies have observed high molecular weight αAAHPs that are likely attributable to the gas-phase reaction of monoterpene SCIs with organic acids.[12–15] Kristensen et al.[14] have proposed that αAAHPs are a major fraction of monoterpene SOA. The reaction of monoterpene SCIs with organic acids can also occur at the air-water interface, such as the surface of cloud droplets and aqueous aerosol. In particular, computational studies have shown that SCIs with hydrophobic substituents are relatively unreactive with water, allowing for reaction with other species, such as acids.[16–18] Recent experimental studies have provided supporting observations, showing that SCIs from monoterpenes and sesquiterpenes give rise to αAAHPs at the air-water interface.[19,20] While these studies suggest the importance of αAAHPs arising from monoterpenes, contradictory results have also been reported. A few studies have found that αAAHPs comprised only a minor fraction of α-pinene SOA extracted in organic or aqueous solvents.[21,22] Such contradictory results reflect the fact that the chem-

istry of αAAHPs has not been investigated in a systematic manner. Unrecognized reactions of αAAHPs are likely occurring in SOA and/or after sample collection.

Multifunctional organic peroxides, such as αAAHPs, comprise a highly complex, unresolved fraction of SOA. These organic peroxide species serve as reservoirs of important oxidants (e.g., the OH radical) and represent a class of reactive oxygen species (ROS), which are linked to adverse health effects of airborne particulate matter.[23,24] Despite their environmental significance, the chemistry of such multifunctional organic peroxides is poorly understood due to their complexity, lack of commercially available standards, and chemical instability. In particular, recent studies have demonstrated the labile nature of particle-bound organic peroxides.[25–27] Other studies have observed formation of H_2O_2 and the OH radical from the water extract of SOA, implying decomposition of larger organic peroxides.[28–30] In this work, two αAAHP species arising from the α-pinene SCIs are synthesized, and their condensed-phase chemistry is investigated for the first time. A specific objective is to understand the behavior of αAAHPs in the aqueous phase, which reflects their fate in cloudwater, aqueous aerosol, and aqueous solvents after extraction. We also attempt to determine the reaction mechanism of the decomposition of αAAHPs, with a particular interest in the extent to which they produce H_2O_2.

Experimental

Liquid Chromatography Electrospray Ionization Mass Spectrometry (LC-ESI-MS)

An LC-ESI-MS technique is used here as the primary analytical method to characterize the synthesized αAAHPs and to monitor their decomposition. The same technique has been employed in a number of our previous studies.[21,31,32] A Waters ACQUITY UPLC I-Class system was coupled to a Quadrupole Time-of-Flight MS (Xevo G2-S QToF). LC separation was performed on an AQUITY BEH C_{18} column (1.7 μm, 2.1 $\times$ 50 mm), with

the column temperature controlled at 30 °C. The injection volume was set at 10 μL, and the flow rate was 0.3 mL min^{-1}. The mobile phase gradient and ESI settings in this study are identical to those in Zhao et al.[21] and will not be discussed with further details here. Leucine enkephalin was employed as the lock mass for accurate mass determination. LC-ESI-MS was operated in both the positive (ESI(+)) and the negative (ESI(-)) modes. Generally, ESI(+) detects oxygenated compounds as ion clusters with Na^+, $NH_4{}^+$, or K^+, while ESI(-) detects compounds containing acidic protons in their deprotonated forms (i.e., as $[M\text{-}H]^-$). In this study, the instrument was operated primarily with ESI(+) as it detects both of the synthesized αAAHPs. ESI(-) was also employed to characterize αAAHPs and to elucidate the reaction mechanisms. Data were acquired and processed with MassLynx v.4.1 software. The reproducibility in the detected peak areas is within 5%, as determined by frequent consistency tests.

Synthesis of αAAHPs

Unless noted otherwise, all chemicals were purchased from Sigma Aldrich without further purification. The synthetic procedure, adapted and modified from that of Witkowski and Gierczak[33], is based on a liquid-phase ozonolysis of α-pinene. The SCIs generated from liquid-phase ozonolysis are forced to form αAAHPs in the presence of an excess amount of an organic acid. The chemical mechanisms behind the synthesis are shown in Figure 2. The synthetic procedure has been described elsewhere.[21] Briefly, α-pinene (50 mM) and an individual organic acid (10 mM) were dissolved in acetonitrile (EMD Millipore). A gentle stream of air (120 sccm) containing approximately 100 ppm of O_3 (generated from a custom-built O_3 generator) was bubbled through the acetonitrile solution. Synthesis of αAAHPs was carried out in an ice bath, and the solutions were stored in a freezer maintained at -16 °C. Two organic acids were selected to synthesize two different αAAHPs. Pinonic acid was selected for its relevance to monoterpene oxidation and its reactivity with SCIs.[14,19] Adipic acid was selected as representative of diacids. The two synthesized αAAHPs are

herein referred to as αAAHP-P, and αAAHP-A, respectively (Figure 2). A synthetic control was also prepared by following the same synthetic procedures, except that no organic acid was added to force the formation of αAAHPs. The synthesized αAAHPs were not further purified due to their chemical instability; therefore, the solutions likely contain byproducts of liquid-phase α-pinene ozonolysis, e.g., through acid-catalyzed tautomerization of SCIs.[34]

Characterization of the Synthesized αAAHPs

The identity of the synthesized αAAHPs was first confirmed with the LC-ESI-MS technique. The synthetic control, αAAHP-A, and αAAHP-P were individually diluted by a factor of 50 to water acidified to pH 2 with H_2SO_4. The purpose of adding H_2SO_4 was to minimize decomposition of αAAHPs, which simplifies their characterization. As will be demonstrated in Results and Discussion, the decomposition of αAAHPs is found to be slow under acidic conditions. The diluted solutions were measured with LC-ESI-MS with both ESI(-) and ESI(+).

Iodometry was employed to confirm the peroxide functionality of αAAHPs. Iodometry is a method that selectively reduces organic peroxides into the corresponding alcohols.[35,36] It has been traditionally employed with UV-Vis spectrometry to quantify the total peroxide content in a sample.[37,38] Our previous work has established a method to couple iodometry to LC-ESI-MS for a molecular-level analysis of organic peroxide; this method has been named iodometry-assisted LC-ESI-MS.[21] In the present work, both of the synthesized αAAHPs were first mixed and diluted by a factor of 50 in an aqueous solution, pre-acidified to pH 2 with H_2SO_4. In this case, acidifying the solution supplies the acid needed for iodometry. The solution was then divided into two aliquots. Potassium iodide (KI, 60 mM) was added to one aliquot to initiate iodometry, while no KI was added to the other aliquot as a control. Both aliquots were kept in the dark at room temperature. LC-ESI-MS measurement with ESI(+) was performed approximately 30 min after the addition of KI.

Hydrolysis of αAAHPs in Condensed Phases

The two αAAHPs were mixed and diluted simultaneously by a factor of 50 in an aqueous solution contained in a plastic LC-ESI-MS sample vial. The emphasis of the current work was placed on hydrolysis in the aqueous phase, but experiments were also performed in methanol and acetonitrile to explore the solvent effects. The sample vial was placed in a temperature-controlled sample holder, and the αAAHP signals were tracked over time using LC-ESI-MS. The temperature in the sample holder was adjusted to 7, 15, 25 and 35 °C to explore the temperature effect. The sample vials and aqueous solutions were preconditioned at the set temperatures before αAAHPs were added. The pH of the αAAHP solution at the default dilution ratio was 4.4 (monitored with a Thermo Scientific pH meter). Its acidity is likely due to the presence of residual pinonic acid and adipic acid used in the synthesis. To investigate the effect of solution pH on the decomposition of αAAHPs, experiments were also conducted in solutions with pH values either adjusted with H_2SO_4/NaOH or buffered with potassium hydrogen phthalate (KHP) (Baker Chemical Co.).

In the ambient atmosphere, αAAHPs are likely present in aqueous phases with highly complex chemical compositions, including numerous organic and inorganic compounds. To account for any matrix effect, we have also performed αAAHP hydrolysis experiments in an aqueous extract of SOA, generated from the reaction of O_3 and α-pinene in the Caltech PhotoOxidation flow Tube (CPOT) reactor.[39] The details of SOA generation, extraction, and characterization are provided in our previous work.[21] Briefly, α-pinene (175 ppb) and O_3 (1 ppm) were mixed in the CPOT in the absence of light, NO_x, and OH scavengers. The experiments were performed at room temperature and under dry conditions (RH $< 10\%$). The average residence time in the CPOT was 3.5 min. Ammonium sulfate ($(NH_4)_2SO_4$) (Mallinckrodt Chemicals) seed aerosol was injected to assist formation of SOA and to minimize vapor-wall interactions. SOA generated in the CPOT was collected on a Teflon filter over 16 hours. The filter was extracted to water by being mechanically shaken for 10 min, immediately before the hydrolysis experiments.

The pH of the SOA extract with diluted αAAHPs was measured to be 4.2. The $(NH_4)_2SO_4$ concentration, arising from the $(NH_4)_2SO_4$ seed aerosol, was approximately 200 μM, semi-quantitatively determined by comparing the peak area of HSO_4^- observed by LC-ESI-MS to those from standard solutions of $(NH_4)_2SO_4$. The total organic carbon (TOC) in the water extract of SOA was measured to be 31 parts per million carbon (ppmC) using a TOC analyzer (OI Analytical, Aurora model 1030w). The accuracy of the TOC instrument was within 5%.

High Performance Liquid Chromatography with Fluorescence Detection (HPLC-Fluorescence)

The formation of H_2O_2 from αAAHPs was monitored with a HPLC-Fluorescence instrument (Shimadzu RF-10AXL) located at the University of California-Los Angeles.[30,40–43] The technique is based on an LC separation of H_2O_2 and organic peroxides on a C_{18} reversed-phase column (GL Science Inc., 5 μm, 4.6 $\times$ 250 mm), followed by a post-column addition of a fluorescent reagent consisted of horseradish peroxidase (HRP) and *p*-hydroxyphenyl acetic acid (PHOPAA). With the catalytic assistance of HRP, PHOPAA selectively reacts with H_2O_2 and organic peroxides to form a fluorescent dimer, which was detected with a fluorescent detector. The excitation and emission wavelengths were set at 320 and 400 nm, respectively. The LC separation is based on an isocratic method with a 100% aqueous mobile phase containing 1 mM of H_2SO_4 (Fisher, 0.1 N, reagent grade) and 0.1 mM of ethylenediaminetetraacetic acid (EDTA) at a total flow rate of 0.6 mL min^{-1}. The length of the LC method was 10 min. The current LC method is optimized for the detection of H_2O_2 and polar organic peroxides. A pulse of acetonitrile (200 μL) was injected 3 min after the sample injection to facilitate the elution of less polar organic peroxides. The synthesized αAAHPs did not elute from the column and were not detected.

For the hydrolysis experiments, αAAHP-A or αAAHP-P was diluted by a factor of 250 in water and stored in the dark at room temperature. Aliquots (20 μL) of the experimental

solution were injected to the HPLC-Fluorescence instrument to monitor the formation of H_2O_2. The method was calibrated against standard H_2O_2 solutions, produced by diluting a commercial H_2O_2 solution (50% in water). The detection limit of the method was 10 nM. We have also performed control experiments in which the synthesized αAAHPs were diluted to the same ratio but in acetonitrile instead of water.

Results and Discussion

Characterization of the Synthesized αAAHPs

Figure 3 shows the base peak intensity (BPI) chromatograms of the synthetic control, αAAHP-A, and αAAHP-P obtained with LC-ESI-MS. BPI chromatograms display the most intense peak at each given retention time (RT). Neither ESI(-) nor ESI(+) has detected any major compounds in the synthetic control (Figure 3a). αAAHPs are detected by both ESI(-) and ESI(+) (Figure 3b and c), and the agreement between the detected and exact masses (Figure 2) is within $\pm$ 10 ppm.

αAAHP-A emerges at RT = 5.8 min and is detected as $[M\text{-}H]^-$ (m/z 329) and $[2M\text{-}H]^-$ (m/z 659) by ESI(-). Along with αAAHP-A, residual adipic acid was also detected by ESI(-) at RT = 3.4 min, primarily as $[M\text{-}H]^-$ (m/z 145). ESI(+) detects αAAHP-A primarily as $[M{+}NH_4]^+$ (m/z 348), but also as $[M{+}Na]^+$ (m/z 353) and $[M{+}K]^+$ (m/z 369). Small organic acids, such as adipic acid, are not efficiently detected as $[M{+}Na]^+$ or $[M{+}NH_4]^+$. In fact, adipic acid is detected by ESI(+) primarily at m/z 346, which corresponds to a complex with iron ($[Fe^{3+}\cdot(M^-)_2]^-$). Iron is likely present at the ESI source or the injection system. We have confirmed that the isotope profile of this peak agrees with that of iron and that the peak area of m/z 346 is proportional to the adipic acid concentration. αAAHP-P (RT = 7 min) does not have any carboxylic groups and is not detected as $[M\text{-}H]^-$ by ESI(-), but instead as a fragment at m/z 183. The precursor of αAAHP-P, pinonic acid, is detected primarily as $[M\text{-}H]^-$ (m/z 183) by ESI(-) at RT = 4.9 min. Similar to the case of

αAAHP-A, αAAHP-P is detected by ESI(+) primarily as $[M+NH_4]^+$ (m/z 386), but also as $[M+Na]^+$ (m/z 391) and $[M+K]^+$ (m/z 407). ESI(+) detects pinonic acid primarily in a dehydrated form, $[M+H\text{-}H_2O]^+$ (m/z 167), but also as the iron complex ($[Fe^{3+}\cdot(M^-)_2]^-$) at m/z 422, similar to the case of adipic acid. Besides the peaks of αAAHPs and their precursor organic acids, ESI(+) has detected a number of minor peaks likely attributable to byproducts arising from the current synthetic procedure. These byproducts do not contain acidic functionalities, as they are not detected by ESI(-).

Figure 4 compares the ESI(+) BPI chromatograms of a mixture of the two αAAHPs treated with and without iodometry. The only major difference between the two BPI chromatograms is a complete attenuation of αAAHP peaks, confirming that they are organic peroxides. Iodometry induced negligible effects on the peaks of synthetic byproducts, indicating that most of these byproducts are non-peroxide species.

Overall, it is confirmed that the synthesized αAAHPs are organic peroxides with the accurate masses and elemental compositions shown in Figure 2. However, we cannot distinguish structural isomers of αAAHPs with the current techniques. As shown in Figure 2a, α-pinene gives rise to two different SCIs, each leading to a distinct αAAHP structural isomer upon reaction with pinonic acid or adipic acid. The characterization also reveals that the αAAHP solutions contain numerous synthetic byproducts. The dominant byproducts are the residual precursor organic acids: adipic acid and pinonic acid. Their concentrations are determined to be approximately 200 μM in the synthetic solution diluted by a factor of 50. Although the majority of byproducts detected by LC-ESI-MS are non-peroxide species, there are likely undetected peroxide species. As will be discussed shortly, the HPLC-fluorescent technique detected a high initial background of H_2O_2, which is too polar to be retained by the LC method used in LC-ESI-MS. The presence of byproducts does not significantly affect the kinetic investigation of αAAHP decomposition, but complicates the interpretation of the reaction mechanisms and will be discussed.

Decay of αAAHPs Signals in Condensed Phases

Figure 5 shows the ESI(+) BPI chromatograms recorded during an example experiment conducted in the aqueous phase at 25 °C with uncontrolled pH (4.4). The chromatograms are color-coded by the time at which each sample is injected to LC-ESI-MS, with that of the first sample defined as time 0. Both of the αAAHP species exhibit rapid decay, while the intensities of other non-peroxide peaks exhibit minimal changes during one hour of reaction time. The inset of Figure 5 shows the 1^{st}-order kinetic plots of the two αAAHPs recorded for the same experiment. The linearity of the plots indicates that the reaction is 1^{st}-order. As discussed in the previous section, αAAHPs are detected by ESI(+) in multiple forms, including $[M+NH_4]^+$, $[M+Na]^+$, and $[M+K]^+$. Each of these three peaks exhibits decay at a very similar rate, and so only the dominant peak $[M+NH_4]^+$ is used for the kinetic analysis. We also conducted an experiment with pimelic acid added to the solution as an internal standard and monitored the signals of αAAHP-A and pimelic acid using ESI(-). The αAAHP-A decay rates with and without the internal standard differed by 8%, which is within the experimental uncertainties; the relative standard deviation of the hydrolysis rate at 25 °C is approximately 15%. As such, all the results discussed here are from experiments without an internal standard.

The effect of solvent on the decay rate of αAAHPs was investigated by performing the experiment at the same dilution ratio and temperature (25 °C), but in methanol and acetonitrile, which are the most commonly employed solvents for filter extraction and analysis. The decay profiles of αAAHP-P in the three solvents are shown in Figure 6. The decay rates of αAAHPs increase in the order of acetonitrile $<$ methanol $<$ water. The results for αAAHP-A exhibit the same trend and are not shown. The 1^{st}-order decay rate coefficients (k^{I}) of αAAHPs and their corresponding e-folding lifetimes (τ_{avg}) in the three solvents are summarized in Table 1. The trend that αAAHPs are more reactive in polar and protic solvents is consistent with hydrolysis. We also note that when αAAHPs are stored in acetonitrile in a freezer maintained at -16 °C, their signals exhibit a slow decay of approximately 25% over

the course of two weeks, indicating that they are highly stable under this condition.

Temperature Effects

The decomposition rates of αAAHPs appear to be highly temperature-dependent. The temperature dependences of the two αAAHPs are shown in Figure 7a, in the format of an Arrhenius plot (i.e., $\ln(k^{\mathrm{I}})$ vs $1/T$). The k^{I} and τ_{avg} values at each temperature are summarized in Table 1. Decomposition of both αAAHPs is accelerated at higher temperatures, with their τ_{avg} values decreasing by roughly an order of magnitude from 7 °C to 35 °C. The slope of the Arrhenius plot is equivalent to $-E_a/R$, where E_a is the activation energy, and R is the gas constant. In this manner, the E_a values for αAAHP-A and αAAHP-P are obtained to be 62.6 ± 4.2 and 60.7 ± 6.7 kJ mol^{-1}, respectively. The uncertainty is obtained from that of the slope. These E_a values are comparable to but larger than those of simple alkyl esters, indicating that hydrolysis of αAAHPs is more sensitive to temperature than that of simple alkyl esters. For instance, E_a values for ethyl formate and diethyl ester are 37.4 and 44.9 kJ mol^{-1}, respectively.[44]

Effects of Solution pH

The effect of solution pH on the decomposition rate of αAAHPs is shown in Figure 7b. All of these experiments were performed at 25 °C. Decomposition of αAAHPs is highly pH dependent, proceeding more rapidly in basic solutions. The solid markers on Figure 7b represent those experiments in which the solution pH was adjusted with either H_2SO_4 or NaOH. These $\log_{10}(k^{\mathrm{I}})$ values exhibit a linear relationship with solution pH, indicating that the rate coefficients are proportional to the concentration of OH^- from pH 3.5 to 5.1. This is within the typical pH range for ambient cloud and fog waters.[45] The highest solution pH examined here is 5.1, as we found that the decomposition rate was too fast to be quantified by the current LC-ESI-MS method at higher pH values.

If organic acids are generated during decomposition of αAAHPs, the solution pH can

be potentially altered during the course of an experiment. To account for this possibility, we also performed experiments in buffered solutions, and the results are shown in Figure 7b. The pH-dependence is similar in buffered and pH-adjusted solutions, indicated by the identical slopes between the two data series. However, the data of the buffered solutions is shifted up from those of the pH-adjusted solution, indicating more rapid decomposition of αAAHPs in buffers.

Matrix Effect

The faster decay of αAAHPs in buffers is likely the result of a matrix effect, which has also been observed in hydrolysis of other organic compounds.[44] The buffer solutions employed in the current work are generated by mixing KHP and NaOH. The KHP concentration ranges from 0.07 M (pH 5.0 buffer) and 0.1 M (pH 4.1 buffer), and that of NaOH ranges between 0.002 M (pH 5.0 buffer) and 0.03 M (pH 4.1 buffer). To explore the potential effect of Na^+ on hydrolysis of αAAHP, we performed a separate control experiment in which the decomposition of αAAHPs was monitored in an aqueous solution containing 0.015 M of Na_2SO_4. This experiment confirmed that Na^+ and SO_4^{2-} at this concentration do not accelerate the decomposition of αAAHPs. As such, KHP present in the buffers is likely responsible. Although KHP at the mM-level concentration is not atmospherically relevant, the fact that KHP accelerated αAAHP decomposition suggests that dissolved organic compounds in cloudwater may also be able to accelerate the decomposition of αAAHPs.

In the atmosphere, particle-phase αAAHPs are likely introduced into cloud and fog waters when the αAAHP-bearing particle is activated into a droplet, a process referred to as nucleation scavenging.[46] As such, in real cloudwater, αAAHPs are present with many other chemical components. The ideal way to investigate matrix effects of other cloudwater components is to use authentic cloudwater samples.[47,48] In the absence of such samples, we have taken a matrix-matching approach by extracting α-pinene SOA components and $(NH_4)_2SO_4$ into water to create an atmospherically relevant sample matrix. In the SOA extract, the k^{I}

values were determined to be $(6.9 \pm 0.6) \times 10^{-4}$ and $(7.0 \pm 0.4) \times 10^{-4}$ for αAAHP-A and αAAHP-P, respectively. These values are significantly higher than those in water with the same pH (pH 4.2). The corresponding k^{I} values in pH 4.2 water are 3.2×10^{-4} and 3.6×10^{-4}, calculated with the pH-dependent curves shown in Figure 7b. Our results indicate that the presence of SOA compounds has doubled the decomposition rate of αAAHPs. Note that the hydrolysis experiment in the SOA extract was repeated in triplicate, and the uncertainty bars are shown in Figure 7b as a reference for the uncertainty range of this matrix-matching experiment.

As discussed in Experimental, the synthesized solutions contain organic acids and other byproducts. To address the potential effect of the synthetic byproducts on the decomposition rate of αAAHPs, we performed an experiment with the αAAHPs diluted by an extra factor of two from the default dilution ratio (i.e. a dilution factor of 100 instead of 50) to reduce the concentration of byproducts. The k^{I} values obtained at these two dilution ratios agree to within 7%. As hydrolysis, a 1$^{\mathrm{st}}$-order reaction, should not be affected by dilution alone, these results indicate that the effect of organic acids and synthetic byproducts on αAAHP decomposition is relatively small under the current experimental conditions.

The TOC concentration of the SOA water extract was measured to be 31 ppmC. Such a level of TOC is typically observed in polluted fog and cloudwater samples, such as those from Fresno, California and Jeju Island, Korea.[46] We did not further perform a systematic investigation of the effect of each individual organic species on the hydrolysis rate of αAAHPs; it is an interesting direction for future studies.

Proposed Mechanism of αAAHP Decomposition

Base-catalyzed Hydrolysis

We have attempted to derive the reaction mechanism of αAAHP decomposition by monitoring the growth of product peaks using LC-ESI-MS. However, as shown in Figure 5, none of the peaks exhibits significant changes in intensity besides those of the decaying αAAHPs.

The only peaks that exhibit minor, yet consistent growth are those attributable to the precursor organic acids, i.e., adipic acid and pinonic acid. Tracking the growth of these peaks is complicated by the fact that high concentrations of these organic acids are present in the solution as byproducts of the αAAHP synthesis prior to the hydrolysis experiments. Growth of the organic acid peaks is most clearly observed when the decomposition of αAAHPs is more rapid, i.e., in experiments with high temperature or high solution pH. Figure 8a and b show the BPI chromatograms of an αAAHP-A solution during a hydrolysis experiment at 35 °C; the growth of adipic acid is confirmed with both ESI(+) and ESI(-). The growing signal of adipic acid and the decaying signal of αAAHP-A during hydrolysis experiments at 35 °C are shown in Figure 8c. Signals are normalized to those at time = 0 (the first injection) for comparison. The growth of adipic acid is highly variable, but an average growth of 19 ± 9% is observed when αAAHP-A is nearly depleted. This magnitude of growth is larger than the method stability of the LC-ESI-MS (± 5%). Production of pinonic acid from αAAHP-P is also observed, but to a less significant extent: 10 ± 3%. Such a small amount of pinonic acid production is close to the method stability. Our results highlight the importance of further purifying the synthesized αAAHPs in future studies, so that large residual acid signals do not mask signal growth due to αAAHP decomposition.

The observed pH-dependence and formation of organic acids are consistent with a base-catalyzed hydrolysis of αAAHPs, as shown by the case of αAAHP-A in Figure 9. The reaction proceeds via a nucleophilic addition of OH^- to the ester, yielding adipic acid and an α-hydroxyhydroperoxide (αHHP) intermediate that is in equilibrium with the corresponding aldehyde, pinonaldehyde, and H_2O_2.[49,50] The formation of H_2O_2 is qualitatively confirmed with the HPLC-fluorescence technique, with the results shown in Figure 10. As mentioned in Experimental, the synthesized solutions were diluted by a factor of 250 in water before the HPLC-fluorescence measurement. A high initial background of H_2O_2, 3.1 μM from αAAHP-A and 2.5 μM from αAAHP-P, is found in the diluted aqueous solutions. We conducted a control experiment, in which αAAHP-P is diluted in acetonitrile instead of water. A

similar initial H_2O_2 concentration (2.9 μM) is measured, but no further production of H_2O_2 is observed over the course of two hours (Figure 10). The control experiment indicates that the initial H_2O_2 likely arises from the synthesis, and is not due to a rapid production upon dilution in water. The initial background has been subtracted from the results presented in Figure 10. When either αAAHP-A or αAAHP-P is diluted in water, a steady production of H_2O_2 is observed. While αAAHPs are depleted in approximately 1 h (as shown by the LC-ESI-MS results), the production of H_2O_2 continues over a much longer time. The HPLC-fluorescence results are consistent with the proposed mechanism (Figure 9), where αAAHPs are first converted into an αHHP intermediate, which likely generates H_2O_2 over a longer time scale. However, due to the impure nature of the synthesized solution, we cannot rule out the possibility that synthetic byproducts can also give rise to H_2O_2.

The observed base-catalyzed hydrolysis of αAAHPs is unique to aqueous-phase reactions. In fact, gas-phase decomposition of organic peroxides is often acid-catalyzed. Computational studies have shown that organic acids (e.g., formic acid) can form prereaction complexes with organic peroxides in the gas phase and reduce the energy barriers associated with their decomposition.[51,52] Conversely, in the aqueous phase, hydrolysis of αAAHPs is initiated via nucleophilic addition of OH^- to the ester functional group (Figure 9) The dependence of aqueous-phase decomposition on acid-base chemistry thus differentiates aqueous-phase mechanisms from their gas-phase counterparts.

Base-catalyzed hydrolysis in the aqueous phase has also been reported for a related class of organic hydroperoxides, αHHPs. In particular, the hydrolysis rates of hydroxymethyl hydroperoxide (HMP) and bis-(hydroxymethyl) peroxide (BHMP) exhibit a linear relationship with the concentration of HO^- from pH 4 to 6.[53,54] This observation is similar to the case of αAAHPs observed in the current work. In general, hydrolysis reactions can be catalyzed by either acid or base.[44] We did not observe any signs of acid-catalyzed hydrolysis within the pH range studied here (pH 3.5 to 5.1), nor did we perform experiments under highly acidic conditions. However, acid-catalyzed hydrolysis of HMP and BHMP was observed in solu-

tions with pH 1.5 or lower.[54] It will be of interest for future studies to investigate potential acid-catalyzed hydrolysis of αAAHPs in highly acidic solutions.

Other Potential Reaction Mechanisms

Besides the base-catalyzed hydrolysis mechanism, a number of other potential mechanisms have been proposed in previous work. The first mechanism is acid anhydride formation via loss of water from αAAHPs (Figure 11a). Studies of gas-phase ozonolysis of ethene in the presence of formic acid have observed the formation of formic acid anhydride, which likely arises from this reaction pathway.[7,55] A computational study[52] has shown that the presence of a third molecule, e.g., an organic acid, serves as the carrier of hydrogen and can efficiently lower the energy barrier of this reaction pathway. As shown in Figure 11a, the acid anhydride arising from αAAHP-A should undergo hydrolysis in the aqueous phase and give rise to pinonic acid and adipic acid. However, pinonic acid, which would have appeared at $RT = 4.9$ min, is not observed in the αAAHP-A hydrolysis experiments (Figure 8a and b). Our results indicate that the acid anhydride pathway is unlikely a major reaction mechanism.

The second reaction pathway considered here involves a cyclization reaction followed by decomposition, a route known as the Korcek mechanism.[56] The Korcek mechanism is particularly relevant to γ-ketohydroperoxides, forming a five-membered cyclic peroxide intermediate, which subsequently decomposes to a carbonyl compound and an organic acid.[57] In particular, Mutzel et al.[38] have proposed that the Korcek mechanism can be responsible for the loss of highly oxidized organic compounds present in SOA. As shown in Figure 11b, the cyclization of αAAHPs represents a special case of the Korcek mechanism, giving rise to a hydroxylated secondary ozonide intermediate. Information on the decomposition pathway of this hydroxylated secondary ozonide intermediate is limited.[58] In the case of αAAHP-A, the Korcek mechanism likely results in two organic acids, pinonic acid and adipic acid for the case of αAAHP-A. As already discussed for the acid anhydride pathway, production of

pinonic acid is not observed in the current work, indicating that the Korcek mechanism is likely a minor reaction pathway.

Conclusion and Environmental Implications

A growing body of work suggests the importance of the reactions between stabilized Criegee intermediates (SCIs) and organic acids in the atmosphere.[5,6,14,18,20] The atmospheric fate of the resulting products, α-acyloxyalkyl hydroperoxides (αAAHPs), needs to be understood for in order to properly assess the environmental importance of SCI + organic acid chemistry. The current study presents the first systematic investigation of the behavior of αAAHPs in the condensed phase. Given a lack of commercially available standards, two αAAHPs were synthesized via liquid-phase ozonolysis of α-pinene. The most significant finding of the current work is a rapid decomposition of αAAHPs in the aqueous phase. The reaction rate is highly dependent on temperature and solution pH, with the observed e-folding lifetimes of αAAHPs ranging from 10 min (at 35 °C or pH 5) to over 100 min (at 7 °C or pH 3.5).

The observations have significant implications for the fate of αAAHPs in the atmosphere. It is now widely accepted that atmospheric aqueous phases, including cloud, fog, and aerosol liquid water, are important reaction media for organic compounds.[59–61] Highly functionalized organic compounds, such as αAAHPs arising from α-pinene ozonolysis, can be introduced into cloud and fog waters through nucleation scavenging. The pH of ambient cloud and fog waters varies between 2 to 7, depending on the chemical composition and the size of the droplets.[45] Larger droplets tend to be less acidic, as they are enriched in species arising from mineral dust and sea salt. Our study shows that base-catalyzed hydrolysis is likely the dominant decomposition pathway of αAAHPs in the cloudwater-relevant pH range. The rapid decay observed in this study implies that αAAHPs can be lost promptly when exposed to cloud and fog with pH values larger than 5. The stability of αAAHPs in aerosol liquid water is dependent on several competing factors and is difficult to predict. The pH values of aerosol

liquid water tend to be lower, typically ranging between -1 to 3.[62] While we did not investigate the behavior of αAAHPs under such acidic conditions, studies on other types of organic hydroperoxide indicate that acid-catalyzed hydrolysis may become dominant in highly acidic solutions.[54] Aerosol liquid water also tends to contain a much higher concentration of organic compounds.[63,64] Observations from the current work show an acceleration of the αAAHP decomposition by dissolved organic compounds generated from α-pinene ozonolysis. The total organic carbon concentration used in the current work is 31 ppmC, equivalent to that in cloud and fog waters from polluted regions. However, extrapolation of the current results to highly complex ambient aerosol liquid water is difficult.

Rapid decomposition of αAAHPs can also occur in laboratory experiments when filter samples are extracted in aqueous or organic solvents. Such loss can potentially explain contradictory results reported in the existing literature regarding the importance of αAAHPs in SOA.[21,22] Based on the kinetic results obtained in this work, key suggestions can be made for future laboratory experiments targeting αAAHPs. Currently, the majority of chemical analyses of SOA components are based on filter collection, extraction, and off-line analyses. Our results suggest that the use of aprotic solvents, such as acetonitrile, can significantly reduce the decomposition of αAAHPs after extraction. If the use of aqueous solvents is unavoidable, the solution should be acidified and stored under lower temperatures to minimize αAAHP decomposition.

The reaction mechanism and the products arising from αAAHP decomposition are also of particular interest in atmospheric chemistry. The observed production of organic acids and H_2O_2 in this work is consistent with a base-catalyzed hydrolysis reaction of αAAHPs. The production of H_2O_2 is particularly important, given that H_2O_2 is a reactive oxygen species and is likely linked to adverse health effects of particulate matter pollution.[23] Formation of H_2O_2 in extracted SOA components has been previously observed and has been attributed to decomposition of larger organic peroxides.[28,30,40] αAAHP may represent one such H_2O_2 source. However, the interpretation of the reaction mechanism in the current work is sig-

nificantly hindered by the presence of organic acids and synthetic byproducts that cannot be easily separated. Currently, we cannot rule out the possibility that H_2O_2 arises from compounds other than αAAHPs. Our results should be confirmed by future studies using pure αAAHP standards. A remaining question for the reaction mechanism of αAAHPs is the cause of their chemical instability. The water extract of α-pinene SOA contains a large number of non-peroxide dimer esters[31,65,66] that are much more stable than αAAHPs and do not exhibit a noticeable decay over a period of days. The hydroperoxide functional group likely introduces the observed chemical lability to αAAHPs, and base-catalyzed hydrolysis alone may not fully explain their rapid decomposition.

Finally, the two αAAHP species studied in this work exhibit similar dependence on all of the experimental conditions examined, implying that a generalized description for the reactivity of αAAHPs may be feasible. The current work focuses on two specific αAAHPs arising from α-pinene SCIs, which does not cover the diversity of SCI-derived organic species in the ambient atmosphere. Future studies should be extended to a wider spectrum of αAAHPs, including those arising from isoprene and other major alkenes.

Acknowledgement

The authors thank Dwight and Christine Landis for their generous contributions and Prof. Paul Wennberg for helpful discussions. LC-ESI-MS and TOC analyses were performed in the Caltech Environmental Analysis Center (EAC). This work was supported by National Science Foundation grants AGS-1523500 and CHE-1508526. RZ also acknowledges support from Natural Science and Engineering Research Council of Canada Post-doctoral Fellowship (NSERC-PDF).

References

(1) Guenther, A.; Hewitt, C. N.; Erickson, D.; Fall, R.; Geron, C.; Graedel, T.; Harley, P.; Klinger, L.; Lerdau, M.; Mckay, W. A. et al. A global model of natural volatile organic compound emissions. *J. Geophys. Res. Atmos.* **1995**, *100*, 8873–8892.

(2) Seinfeld, J. H.; Pandis, S. N. *Atmospheric Chemistry and Physics: From Air Pollution to Climate Change*, 3rd ed.; John Wiley & Sons, Hoboken, New Jersey, 2016.

(3) Criegee, R. Mechanism of ozonolysis. *Angew. Chem. Int. Ed.* **1975**, *14*, 745–752.

(4) Osborn, D. L.; Taatjes, C. A. The physical chemistry of Criegee intermediates in the gas phase. *Int. Rev. Phys. Chem.* **2015**, *34*, 309–360.

(5) Taatjes, C. A.; Shallcross, D. E.; Percival, C. J. Research frontiers in the chemistry of Criegee intermediates and tropospheric ozonolysis. *Phys. Chem. Chem. Phys.* **2014**, *16*, 1704–1718.

(6) Welz, O.; Eskola, A. J.; Sheps, L.; Rotavera, B.; Savee, J. D.; Scheer, A. M.; Osborn, D. L.; Lowe, D.; Murray Booth, A.; Xiao, P. et al. Rate coefficients of C1 and C2 Criegee intermediate reactions with formic and acetic acid near the collision limit: direct kinetics measurements and atmospheric implications. *Angew. Chem. Int. Ed.* **2014**, *53*, 4547–4550.

(7) Neeb, P.; Horie, O.; Moortgat, G. K. Gas-phase ozonolysis of ethene in the presence of hydroxylic compounds. *Int. J. Chem. Kinet.* **1996**, *28*, 721–730.

(8) Tobias, H. J.; Ziemann, P. J. Kinetics of the gas-phase reactions of alcohols, aldehydes, carboxylic acids, and water with the C13 stabilized Criegee intermediate formed from ozonolysis of 1-tetradecene. *J. Phys. Chem. A* **2001**, *105*, 6129–6135.

(9) Stone, D.; Blitz, M.; Daubney, L.; Howes, N. U.; Seakins, P. Kinetics of CH_2OO reac-

tions with SO_2, NO_2, NO, H_2O and CH_3CHO as a function of pressure. *Phys. Chem. Chem. Phys.* **2014**, *16*, 1139–1149.

(10) Mochida, M.; Katrib, Y.; Jayne, J. T.; Worsnop, D. R.; Martin, S. T. The relative importance of competing pathways for the formation of high-molecular-weight peroxides in the ozonolysis of organic aerosol particles. *Atmos. Chem. Phys.* **2006**, *6*, 4851–4866.

(11) Sakamoto, Y.; Inomata, S.; Hirokawa, J. Oligomerization reaction of the criegee intermediate leads to secondary organic aerosol formation in ethylene ozonolysis. *J. Phys. Chem. A* **2013**, *117*, 12912–12921.

(12) Kristensen, K.; Enggrob, K. L.; King, S. M.; Worton, D. R.; Platt, S. M.; Mortensen, R.; Rosenoern, T.; Surratt, J. D.; Bilde, M.; Goldstein, A. H. et al. Formation and occurrence of dimer esters of pinene oxidation products in atmospheric aerosols. *Atmos. Chem. Phys.* **2013**, *13*, 3763–3776.

(13) Kristensen, K.; Cui, T.; Zhang, H.; Gold, A.; Glasius, M.; Surratt, J. D. Dimers in α-pinene secondary organic aerosol: effect of hydroxyl radical, ozone, relative humidity and aerosol acidity. *Atmos. Chem. Phys.* **2014**, *14*, 4201–4218.

(14) Kristensen, K.; Watne, A. K.; Hammes, J.; Lutz, A.; Petäjä, T.; Hallquist, M.; Bilde, M.; Glasius, M. High-molecular weight dimer esters are major products in aerosols from α-pinene ozonolysis and the boreal forest. *Environ. Sci. Technol. Lett.* **2016**, *3*, 280–285.

(15) Kristensen, K.; Jensen, L.; Glasius, M.; Bilde, M. The effect of sub-zero temperature on the formation and composition of secondary organic aerosol from ozonolysis of α-pinene. *Environ. Sci. Processes Impacts* **2017**, *19*, 1220–1234.

(16) Zhu, C.; Kumar, M.; Zhong, J.; Li, L.; Francisco, J. S.; Zeng, X. C. New mechanistic pathways for Criegee–water chemistry at the air/water interface. *J. Ame. Chem. Soc.* **2016**, *138*, 11164–11169.

(17) Zhong, J.; Kumar, M.; Zhu, C. Q.; Francisco, J. S.; Zeng, X. C. Surprising stability of larger Criegee intermediates on aqueous interfaces. *Angew. Chem. Int. Ed.* **2017**, *56*, 7740–7744.

(18) Kumar, M.; Zhong, J.; Zeng, X. C.; Francisco, J. S. Reaction of Criegee intermediate with nitric acid at the air–water interface. *J. Ame. Chem. Soc.* **2018**, *140*, 4913–4921.

(19) Enami, S.; Colussi, A. J. Efficient scavenging of Criegee intermediates on water by surface-active cis-pinonic acid. *Phys. Chem. Chem. Phys.* **2017**, *19*, 17044–17051.

(20) Enami, S.; Colussi, A. J. Criegee chemistry on aqueous organic surfaces. *J. Phys. Chem. Lett.* **2017**, *8*, 1615–1623.

(21) Zhao, R.; Kenseth, C. M.; Huang, Y.; Dalleska, N. F.; Seinfeld, J. H. Iodometry-assisted liquid chromatography electrospray ionization mass spectrometry for analysis of organic peroxides - an application to atmospheric secondary organic aerosol. *Environ. Sci. Technol.* **2018**, *52*, 2108–2117.

(22) Witkowski, B.; Gierczak, T. Early stage composition of SOA produced by α-pinene/ozone reaction: α-Acyloxyhydroperoxy aldehydes and acidic dimers. *Atmos. Environ.* **2014**, *95*, 59–70.

(23) Tao, F.; Gonzalez-Flecha, B.; Kobzik, L. Reactive oxygen species in pulmonary inflammation by ambient particulates. *Free Radical Biol. Med.* **2003**, *35*, 327–340.

(24) Shiraiwa, M.; Ueda, K.; Pozzer, A.; Lammel, G.; Kampf, C. J.; Fushimi, A.; Enami, S.; Arangio, A. M.; Fröhlich-Nowoisky, J.; Fujitani, Y. et al. Aerosol health effects from molecular to global scales. *Environ. Sci. Technol.* **2017**, *51*, 13545–13567.

(25) Krapf, M.; El Haddad, I.; Bruns, E. A.; Molteni, U.; Daellenbach, K. R.; Prévôt, A. S.; Baltensperger, U.; Dommen, J. Labile peroxides in secondary organic aerosol. *Chem* **2016**, *1*, 603–616.

(26) Li, H.; Chen, Z.; Huang, L.; Huang, D. Organic peroxides' gas-particle partitioning and rapid heterogeneous decomposition on secondary organic aerosol. *Atmos. Chem. Phys.* **2016**, *16*, 1837–1848.

(27) Riva, M.; Budisulistiorini, S. H.; Zhang, Z.; Gold, A.; Thornton, J. A.; Turpin, B. J.; Surratt, J. D. Multiphase reactivity of gaseous hydroperoxide oligomers produced from isoprene ozonolysis in the presence of acidified aerosols. *Atmos. Environ.* **2017**, *152*, 314 – 322.

(28) Badali, K. M.; Zhou, S.; Aljawhary, D.; Antiñolo, M.; Chen, W. J.; Lok, A.; Mungall, E.; Wong, J. P. S.; Zhao, R.; Abbatt, J. P. D. Formation of hydroxyl radicals from photolysis of secondary organic aerosol material. *Atmos. Chem. Phys.* **2015**, *15*, 7831–7840.

(29) Tong, H.; Arangio, A. M.; Lakey, P. S. J.; Berkemeier, T.; Liu, F.; Kampf, C. J.; Brune, W. H.; Pöschl, U.; Shiraiwa, M. Hydroxyl radicals from secondary organic aerosol decomposition in water. *Atmos. Chem. Phys.* **2016**, *16*, 1761–1771.

(30) Arellanes, C.; Paulson, S. E.; Fine, P. M.; Sioutas, C. Exceeding of Henry's law by hydrogen peroxide associated with urban aerosols. *Environ. Sci. Technol.* **2006**, *40*, 4859–4866.

(31) Zhang, X.; McVay, R. C.; Huang, D. D.; Dalleska, N. F.; Aumont, B.; Flagan, R. C.; Seinfeld, J. H. Formation and evolution of molecular products in α-pinene secondary organic aerosol. *Proc. Natl. Acad. Sci. U.S.A.* **2015**, *112*, 14168–14173.

(32) Zhang, X.; Dalleska, N. F.; Huang, D. D.; Bates, K. H.; Sorooshian, A.; Flagan, R. C.; Seinfeld, J. H. Time-resolved molecular characterization of organic aerosols by PILS+ UPLC/ESI-Q-TOFMS. *Atmos. Environ.* **2015**, *130*, 180–189.

(33) Witkowski, B.; Gierczak, T. Analysis of α-acyloxyhydroperoxy aldehydes with electrospray ionization-tandem mass spectrometry (ESI-MS(n)). *J. Mass Spectrom.* **2013**, *48*, 79–88.

(34) Kumar, M.; Busch, D. H.; Subramaniam, B.; Thompson, W. H. Barrierless tautomerization of Criegee intermediates via acid catalysis. *Phys. Chem. Chem. Phys.* **2014**, *16*, 22968–22973.

(35) Banerjee, D. K.; Budke, C. C. Spectrophotometric determination of traces of peroxides in organic solvents. *Anal. Chem.* **1964**, *36*, 792–796.

(36) Bloomfield, M. The spectrophotometric determination of hydroperoxide and peroxide in a lipid pharmaceutical product by flow injection analysis. *Analyst* **1999**, *124*, 1865–1871.

(37) Docherty, K. S.; Wu, W.; Lim, Y. B.; Ziemann, P. J. Contributions of organic peroxides to secondary aerosol formed from reactions of monoterpenes with O_3. *Environ. Sci. Technol.* **2005**, *39*, 4049–4059.

(38) Mutzel, A.; Poulain, L.; Berndt, T.; Iinuma, Y.; Rodigast, M.; Böge, O.; Richters, S.; Spindler, G.; Sipilä, M.; Jokinen, T. et al. Highly oxidized multifunctional organic compounds observed in tropospheric particles: a field and laboratory study. *Environ. Sci. Technol.* **2015**, *49*, 7754–7761.

(39) Huang, Y.; Coggon, M. M.; Zhao, R.; Lignell, H.; Bauer, M. U.; Flagan, R. C.; Seinfeld, J. H. The Caltech Photooxidation Flow Tube reactor: design, fluid dynamics and characterization. *Atmos. Mea. Tech.* **2017**, *10*, 839–867.

(40) Wang, Y.; Kim, H.; Paulson, S. E. Hydrogen peroxide generation from α- and β-pinene and toluene secondary organic aerosols. *Atmos. Environ.* **2011**, *45*, 3149 – 3156.

(41) Wang, Y.; Arellanes, C.; Paulson, S. E. Hydrogen peroxide associated with ambient fine-mode, diesel, and biodiesel aerosol particles in Southern California. *Aerosol Sci. Technol.* **2012**, *46*, 394–402.

(42) Hasson, A. S.; Orzechowska, G.; Paulson, S. E. Production of stabilized Criegee intermediates and peroxides in the gas phase ozonolysis of alkenes: 1. Ethene, trans-2-butene, and 2,3-dimethyl-2-butene. *J. Geophys. Res. Atmos.* **2001**, *106*, 34131–34142, doi:10.1029/2001JD000597.

(43) Hasson, A. S.; Ho, A. W.; Kuwata, K. T.; Paulson, S. E. Production of stabilized Criegee intermediates and peroxides in the gas phase ozonolysis of alkenes: 2. Asymmetric and biogenic alkenes. *J. Geophys. Res. Atmos.* **2001**, *106*, 34143–34153, doi:10.1029/2001JD000598.

(44) Mabey, W.; Mill, T. Critical review of hydrolysis of organic compounds in water under environmental conditions. *J. Phys. Chem. Ref. Data* **1978**, *7*, 383–415.

(45) Collett, J. L.; Bator, A.; Rao, X.; Demoz, B. B. Acidity variations across the cloud drop size spectrum and their influence on rates of atmospheric sulfate production. *Geophys. Res. Lett.* **1994**, *21*, 2393–2396, doi:10.1029/94GL02480.

(46) Herckes, P.; Valsaraj, K. T.; Collett Jr, J. L. A review of observations of organic matter in fogs and clouds: origin, processing and fate. *Atmos. Res.* **2013**, *132*, 434–449.

(47) Boris, A. J.; Desyaterik, Y.; Collett, J. L. How do components of real cloud water affect aqueous pyruvate oxidation? *Atmos. Res.* **2014**, *143*, 95 – 106.

(48) Lee, A. K. Y.; Herckes, P.; Leaitch, W. R.; Macdonald, A. M.; Abbatt, J. P. D. Aqueous OH oxidation of ambient organic aerosol and cloud water organics: Formation of highly oxidized products. *Geophys. Res. Lett. 38*, doi:10.1029/2011GL047439.

(49) Zhao, R.; Lee, A. K. Y.; Abbatt, J. P. D. Investigation of aqueous-phase photooxidation of glyoxal and methylglyoxal by aerosol chemical ionization mass spectrometry: observation of hydroxyhydroperoxide formation. *J. Phys. Chem. A* **2012**, *116*, 6253–6263.

(50) Zhao, R.; Lee, A. K. Y.; Soong, R.; Simpson, A. J.; Abbatt, J. P. D. Formation of aqueous-phase α-hydroxyhydroperoxides (α-HHP): potential atmospheric impacts. *Atmos. Chem. Phys.* **2013**, *13*, 5857–5872.

(51) Kumar, M.; Busch, D. H.; Subramaniam, B.; Thompson, W. H. Role of tunable acid catalysis in decomposition of α-hydroxyalkyl hydroperoxides and mechanistic implications for tropospheric chemistry. *J. Phys. Chem. A* **2014**, *118*, 9701–9711.

(52) Aplincourt, P.; Ruiz-López, M. F. Theoretical study of formic acid anhydride formation from carbonyl oxide in the atmosphere. *J. Phys. Chem. A* **2000**, *104*, 380–388.

(53) Zhou, X.; Lee, Y. N. Aqueous solubility and reaction kinetics of hydroxymethyl hydroperoxide. *J. Phys. Chem.* **1992**, *96*, 265–272.

(54) Marklund, S. Simultaneous determination of bis (hydroxymethyl)-peroxide (BHMP), hydroxymethylhydroperoxide (HMP), and H_2O_2 with titanium (IV)-equilibria between peroxides and stabilities of HMP and BHMP at physiological conditions. *Acta Chem. Scand.* **1971**, *25*, 3517.

(55) Neeb, P.; Horie, O.; Moortgat, G. K. The nature of the transitory product in the gas-phase ozonolysis of ethene. *Chem. Phys. Lett.* **1995**, *246*, 150 – 156.

(56) Jensen, R. K.; Korcek, S.; Mahoney, L. R.; Zinbo, M. Liquid-phase autoxidation of organic compounds at elevated temperatures. 2. Kinetics and mechanisms of the formation of cleavage products in n-hexadecane autoxidation. *J. Am. Chem. Soc.* **1981**, *103*, 1742–1749.

(57) Jalan, A.; Alecu, I. M.; Meana-Pañeda, R.; Aguilera-Iparraguirre, J.; Yang, K. R.; Merchant, S. S.; Truhlar, D. G.; Green, W. H. New pathways for formation of acids and carbonyl products in low-temperature oxidation: the Korcek decomposition of γ-ketohydroperoxides. *J. Am. Chem. Soc.* **2013**, *135*, 11100–11114.

(58) Moshammer, K.; Jasper, A. W.; Popolan-Vaida, D. M.; Lucassen, A.; Dievart, P.; Selim, H.; Eskola, A. J.; Taatjes, C. A.; Leone, S. R.; Sarathy, S. M. et al. Detection and identification of the keto-hydroperoxide ($HOOCH_2OCHO$) and other intermediates during low-temperature oxidation of dimethyl ether. *J. Phys. Chem. A* **2015**, *119*, 7361–7374.

(59) Ervens, B. Modeling the processing of aerosol and trace gases in clouds and fogs. *Chem. Rev.* **2015**, *115*, 4157–4198.

(60) McNeill, V. F. Aqueous organic chemistry in the atmosphere: sources and chemical processing of organic aerosols. *Environ. Sci. Technol.* **2015**, *49*, 1237–1244.

(61) Zhao, R.; Lee, A. K. Y.; Wang, C.; Wania, F.; Wong, J. P. S.; Zhou, S.; Abbatt, J. P. D. *Advances in Atmospheric Chemistry*, 1st ed.; 2017; Chapter 2, pp 95–184.

(62) Murphy, J. G.; Gregoire, P. K.; Tevlin, A. G.; Wentworth, G. R.; Ellis, R. A.; Markovic, M. Z.; VandenBoer, T. C. Observational constraints on particle acidity using measurements and modelling of particles and gases. *Faraday Discuss.* **2017**, *200*, 379–395.

(63) Arakaki, T.; Anastasio, C.; Kuroki, Y.; Nakajima, H.; Okada, K.; Kotani, Y.; Handa, D.; Azechi, S.; Kimura, T.; Tsuhako, A. et al. A general scavenging rate constant for reaction of hydroxyl radical with organic carbon in atmospheric waters. *Environ. Sci. Technol.* **2013**, *47*, 8196–8203.

(64) Volkamer, R.; Ziemann, P. J.; Molina, M. J. Secondary organic aerosol formation from acetylene (C_2H_2): seed effect on SOA yields due to organic photochemistry in the aerosol aqueous phase. *Atmos. Chem. Phys.* **2009**, *9*, 1907–1928.

(65) Yasmeen, F.; Vermeylen, R.; Szmigielski, R.; Iinuma, Y.; Böge, O.; Herrmann, H.; Maenhaut, W.; Claeys, M. Terpenylic acid and related compounds: precursors for

dimers in secondary organic aerosol from the ozonolysis of α-and β-pinene. *Atmos. Chem. Phys.* **2010**, *10*, 9383–9392.

(66) Müller, L.; Reinnig, M.-C.; Warnke, J.; Hoffmann, T. Unambiguous identification of esters as oligomers in secondary organic aerosol formed from cyclohexene and cyclohexene/α-pinene ozonolysis. *Atmos. Chem. Phys.* **2008**, *8*, 1423–1433.

Table 1: Summary of 1st-order decay rates (k^{I}) and corresponding e-folding lifetimes (τ_{avg}) of αAAHPs under a variety of experimental conditions.

			αAAHP-A		αAAHP-P	
Solvent	T (°C)	pH[a]	$k^{\mathrm{I}}(\mathrm{s}^{-1})$[b]	τ_{avg} (min)	$k^{\mathrm{I}}(\mathrm{s}^{-1})$[b]	τ_{avg} (min)
Acetonitrile	25	N.A.	$(1.4 \pm 0.8) \times 10^{-5}$	1200	$(1.3 \pm 0.8) \times 10^{-5}$	1200
Methanol	25	N.A.	$(8.9 \pm 0.3) \times 10^{-5}$	190	$(8.8 \pm 0.2) \times 10^{-5}$	190
SOA	25	4.2	$(6.9 \pm 0.6) \times 10^{-4}$	24	$(7.0 \pm 0.4) \times 10^{-4}$	24
Water	25	4.4	$(5.8 \pm 1.0) \times 10^{-4}$	29	$(4.9 \pm 0.7) \times 10^{-4}$	34
Water	7	4.4	$(1.3 \pm 0.2) \times 10^{-4}$	110	$(1.4 \pm 0.1) \times 10^{-4}$	110
Water	15	4.4	$(2.3 \pm 0.3) \times 10^{-4}$	72	$(2.0 \pm 0.3) \times 10^{-4}$	83
Water	35	4.4	$(1.6 \pm 0.4) \times 10^{-3}$	11	$(1.4 \pm 0.4) \times 10^{-3}$	12

[a] Solution pH was uncontrolled in the listed experiments.
[b] Uncertainties associated with k^{I} are the standard deviation of three replicates.

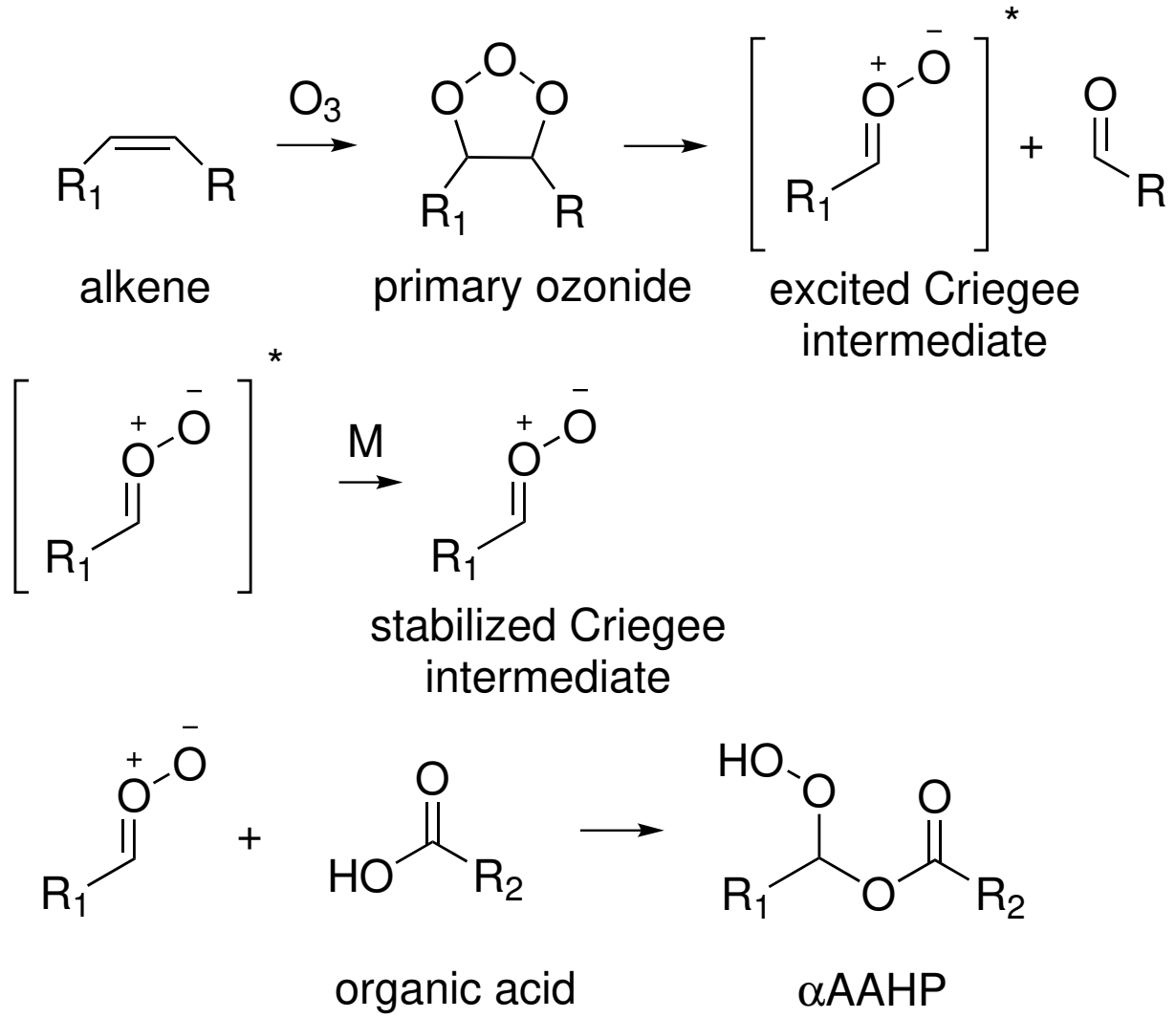

Figure 1: Schematic of the general atmospheric formation mechanism of α-acyloxyalkyl hydroperoxide (αAAHP).

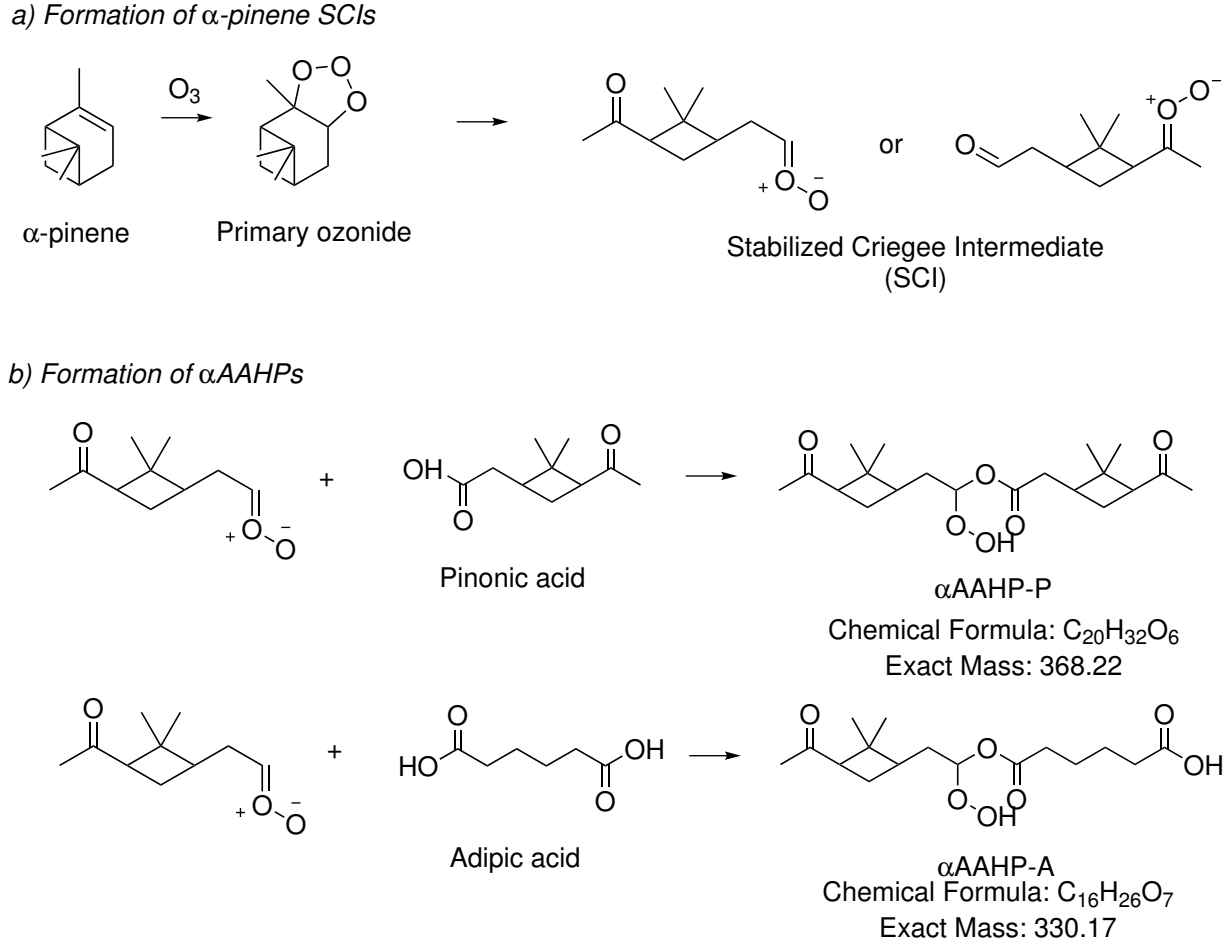

Figure 2: Synthetic pathways and possible structures of αAAHP-P and αAAHP-A. Simplified schematics for a) the formation of α-pinene SCIs, and b) the formation of αAAHPs are shown. Ozonolysis of α-pinene gives rise to two possible SCIs, which subsequently form two αAAHP structural isomers upon reaction with an organic acid. For simplicity, only the αAAHPs arising from one SCI are shown in (b).

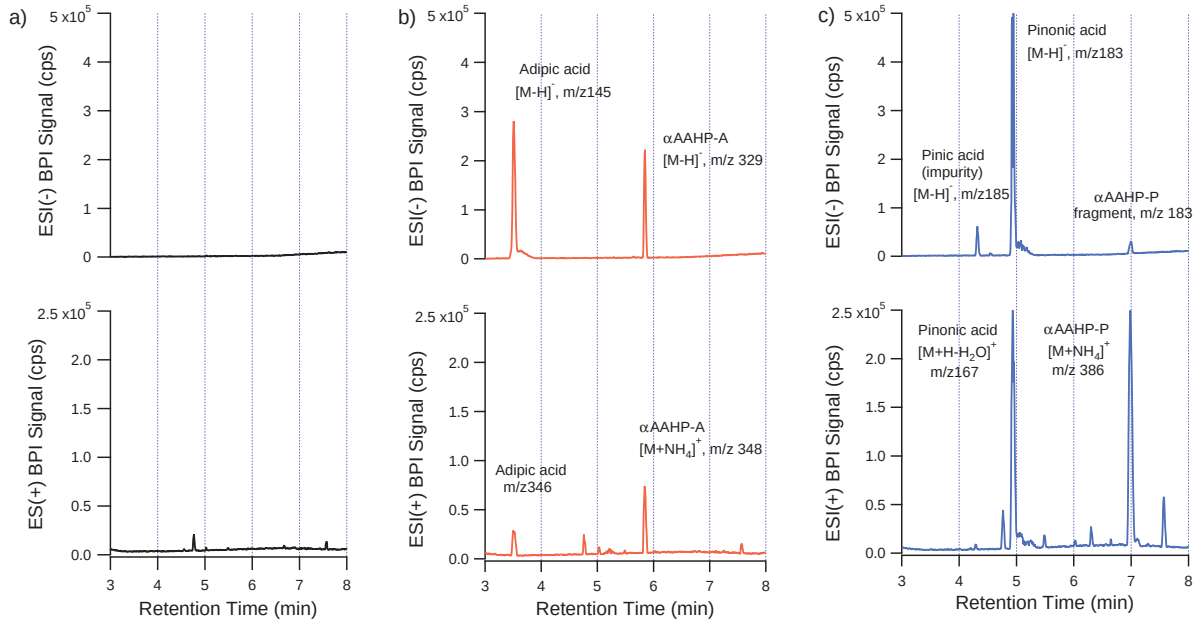

Figure 3: LC-ESI-MS BPI chromatograms of a) the synthetic control, b) αAAHP-A and, c) αAAHP-P. The top panels show the results obtained with ESI(-) and the bottom panels show those obtained with ESI(+).

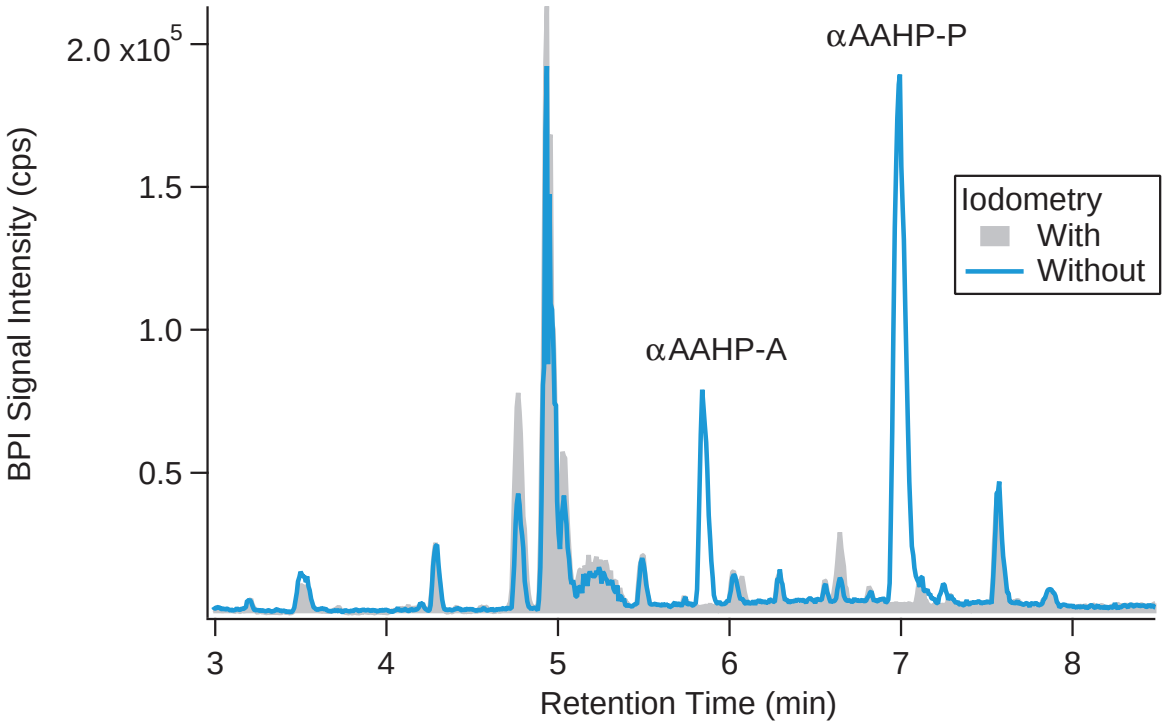

Figure 4: Characterization of the synthesized αAAHPs with iodometry-assisted LC-ESI-MS. ESI(+) BPI chromatograms of an aqueous solution treated with and without iodometry are compared.

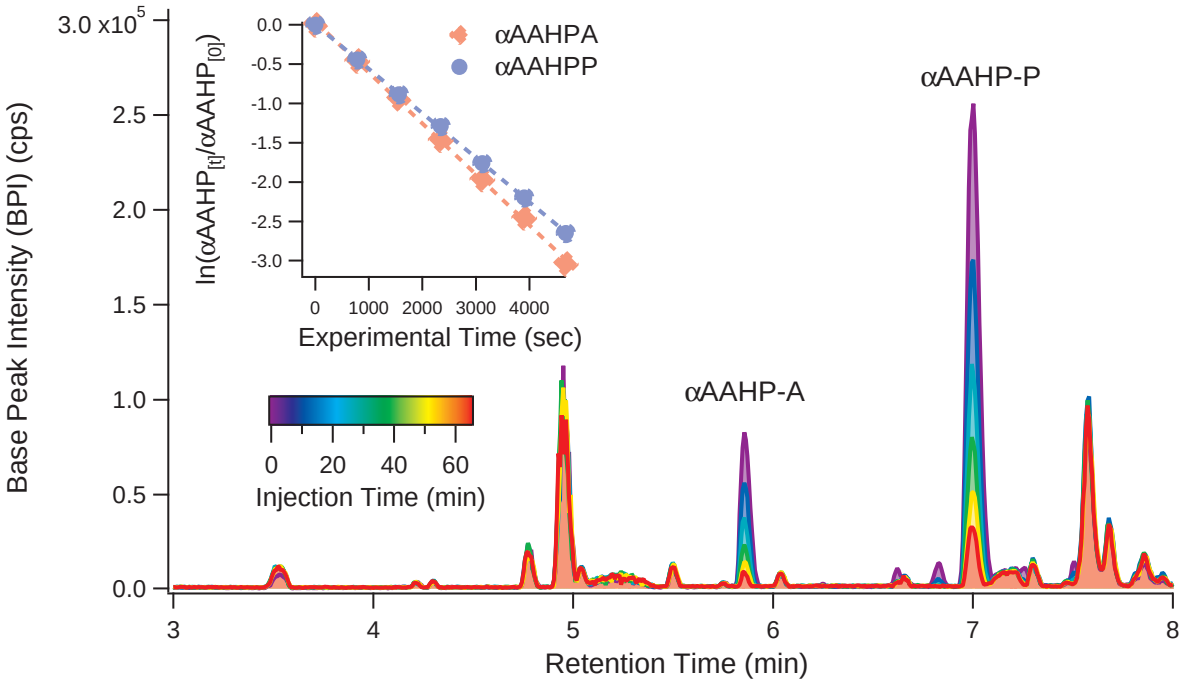

Figure 5: ESI(+) BPI chromatograms recorded in an example experiment at 25 °C with uncontrolled pH (4.4). Chromatograms are color-coded by the time each sample is injected to LC-ESI-MS. Time at which the first sample is injected is defined as time 0. The inset presents the 1st-order kinetic plots of the αAAHPs signal from the same experiment.

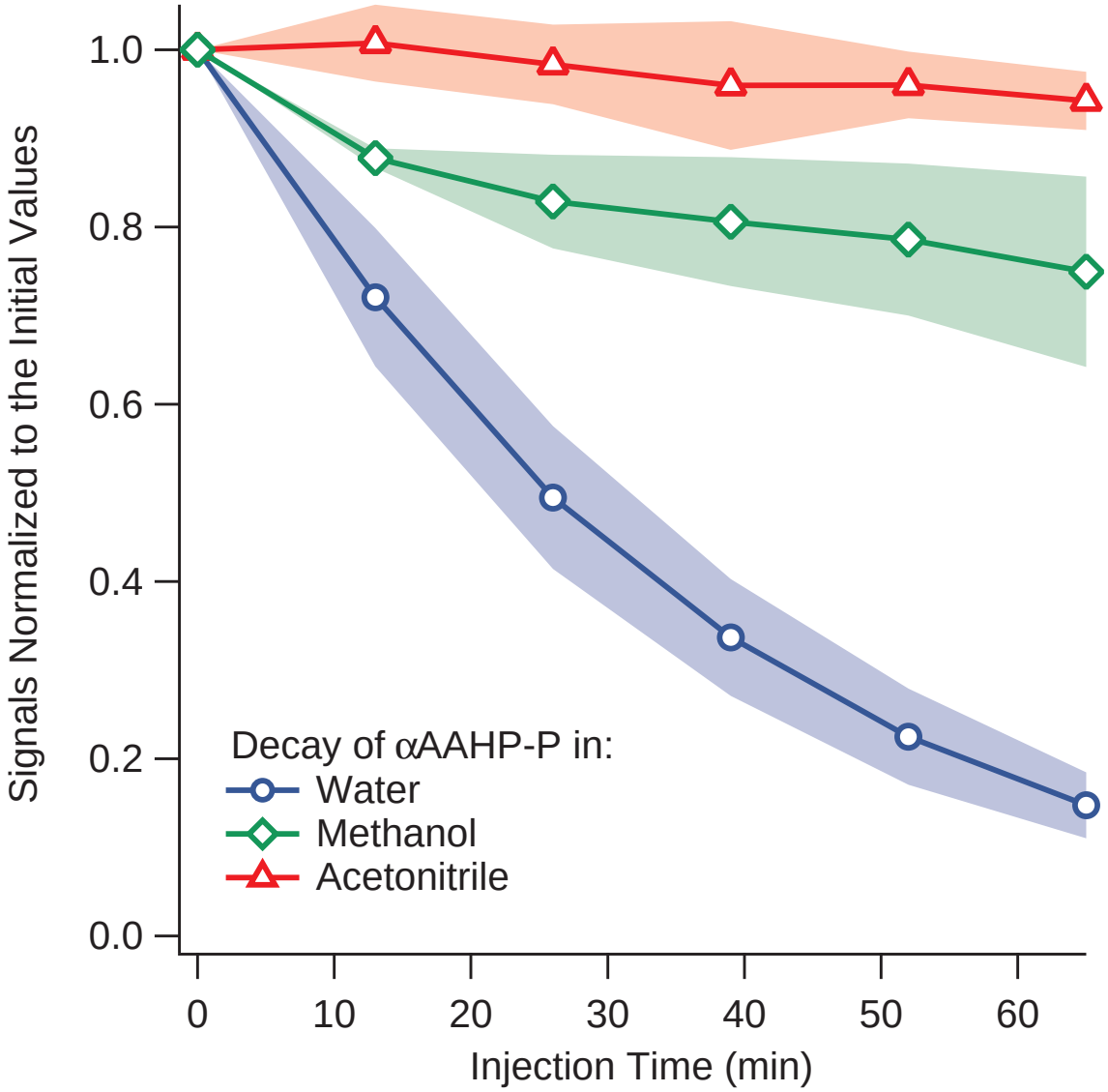

Figure 6: Decay of αAAHP-P in acetonitrile, methanol, and water. Experiments were performed at 25 °C with uncontrolled solution pH. The results represent the average of three replicates, with the error shading indicating one standard deviation.

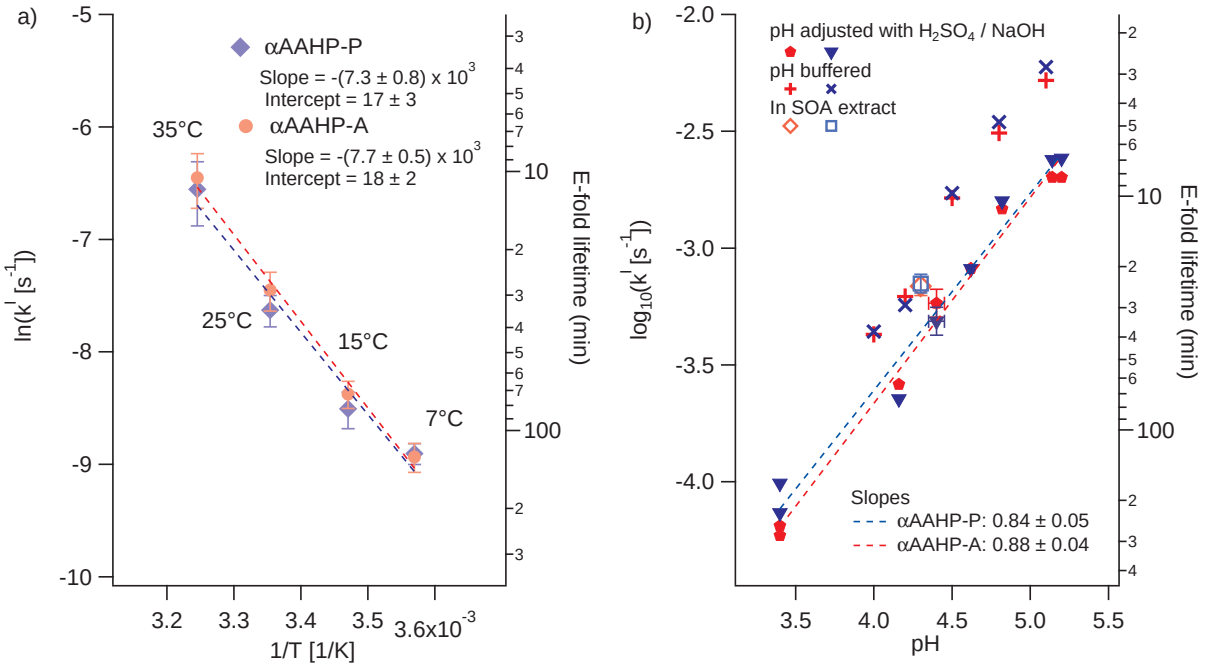

Figure 7: Temperature effect on the 1st-order decay rate of αAAHP (k^{I}), shown in (a) as an Arrhenius plot (i.e., as $\ln(k^I)$ vs. $1/\mathrm{T}$). These experiments were performed with the solution pH uncontrolled (∼4.4). The effects of pH and solution matrix on k^{I} (in the $\log_{10}$ scale) are shown in (b). All of these experiments were performed at 25 °C. Red markers denote αAAHP-A, while blue markers represent αAAHP-P. For both (a) and (b), the corresponding e-folding lifetimes are shown on the right axis. The uncertainty bars, where applicable, represent one standard deviation obtained from triplicate experiments.

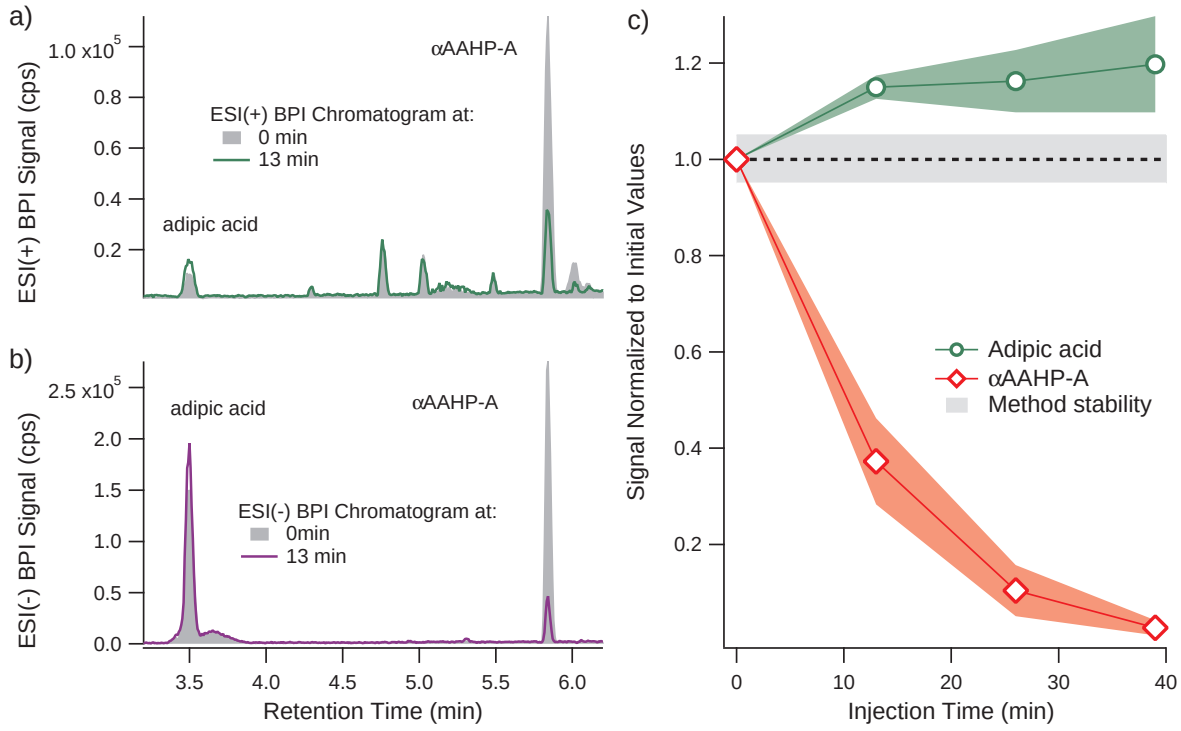

Figure 8: Change of signals in αAAHP-A hydrolysis experiment at 35 °C. The BPI chromatograms obtained with ESI(+) (a) and ESI(-) (b) at 0 min and 13 min injection time are compared. The growth of the adipic acid signal and the decay of αAAHP-A signal as a function of injection time, measured with ESI(+), are shown in (c). Signals are normalized to the values obtained for the first injection, and the uncertainties correspond to the standard deviation of triplicate. The dashed line and the shaded area around it represent the stability ($\pm$ 5%) of the LC-ESI-MS method.

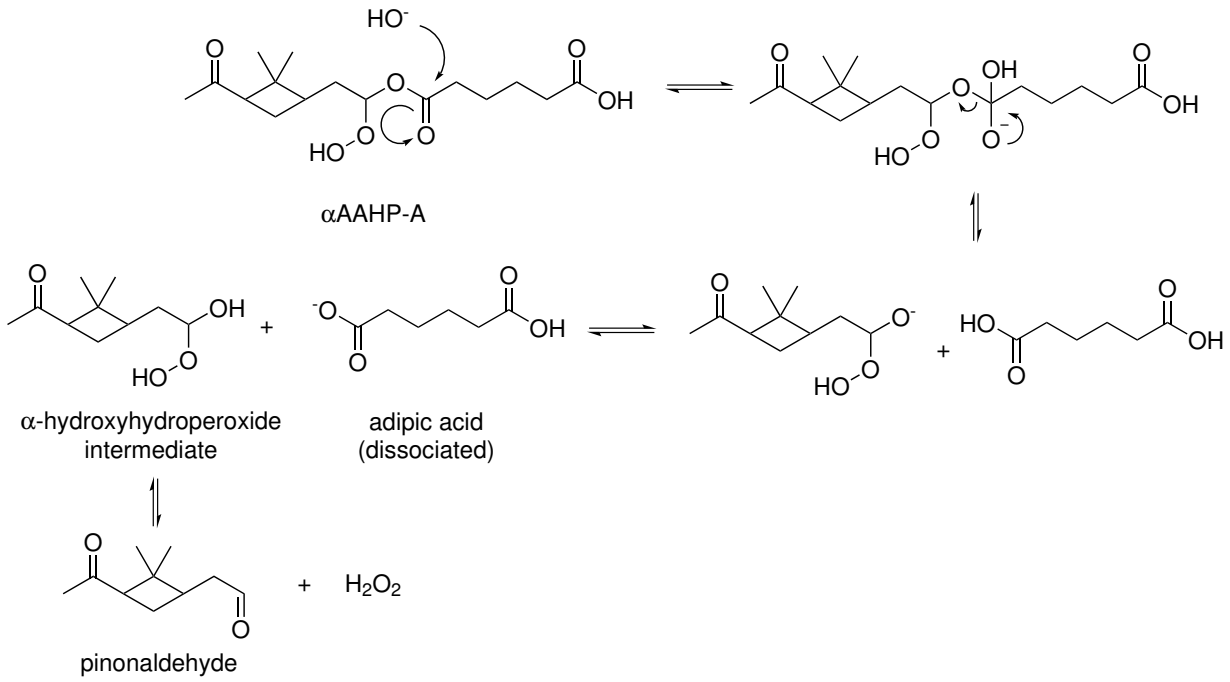

Figure 9: Base-catalyzed hydrolysis of αAAHP. The case of αAAHP-A is shown.

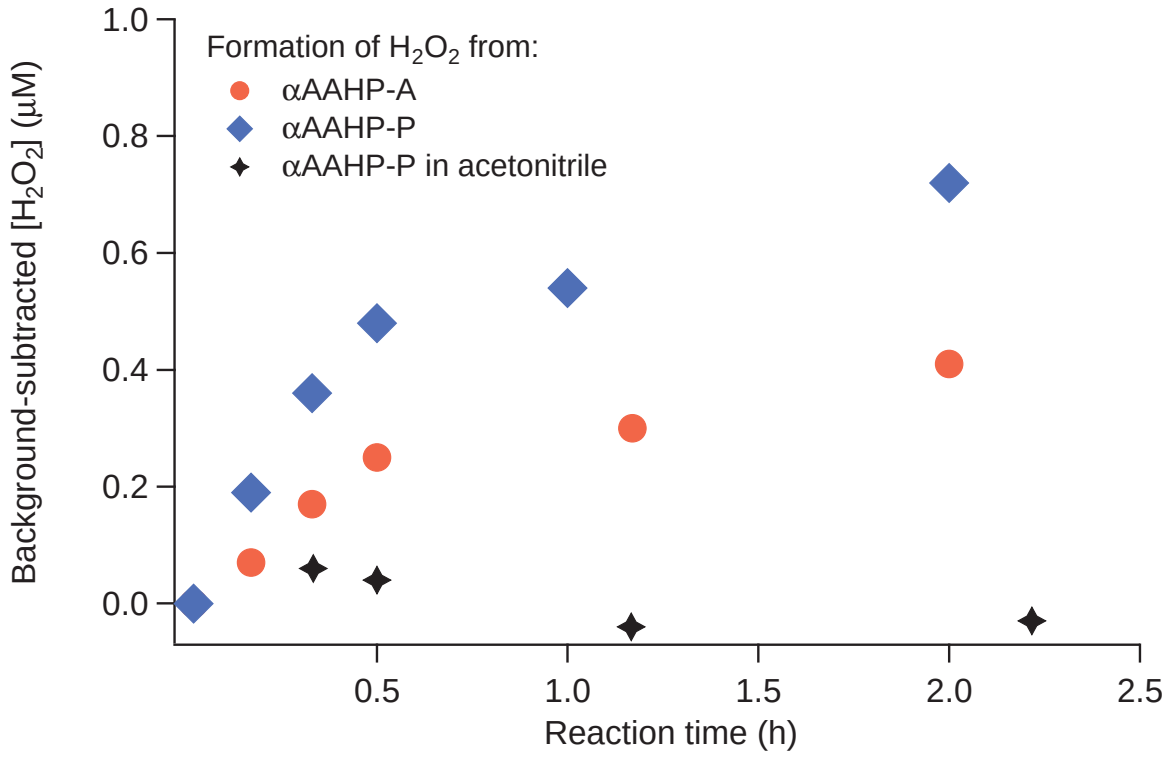

Figure 10: Production of H_2O_2 from αAAHPs diluted in water, measured using HPLC-Fluorescence. The samples contain a high background of H_2O_2 from synthesis, which has been subtracted. The black trace shows the result of a control experiment, where αAAHP-P is dissolved in acetonitrile instead of water.

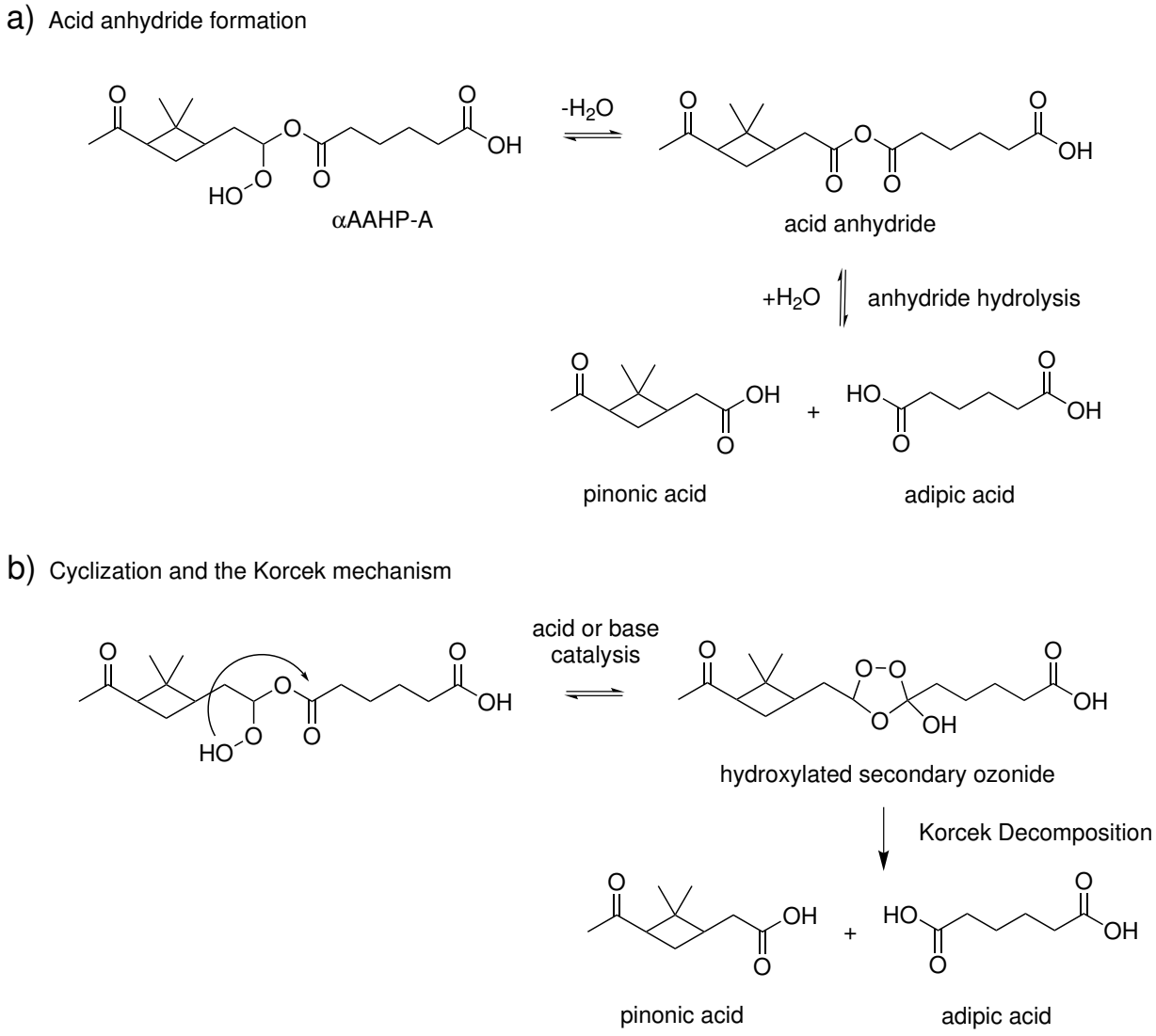

Figure 11: Other potential decomposition mechanisms of αAAHPs: (a) Acid anhydride formation and (b) the Korcek mechanism. The cases for αAAHP-A are shown.

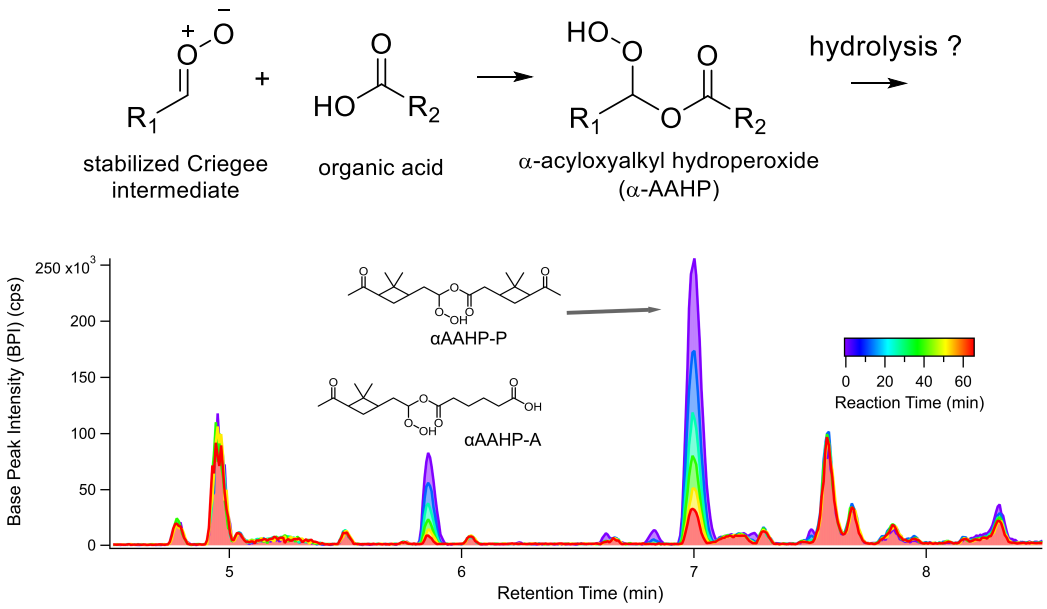

Figure 12: TOC graphic.